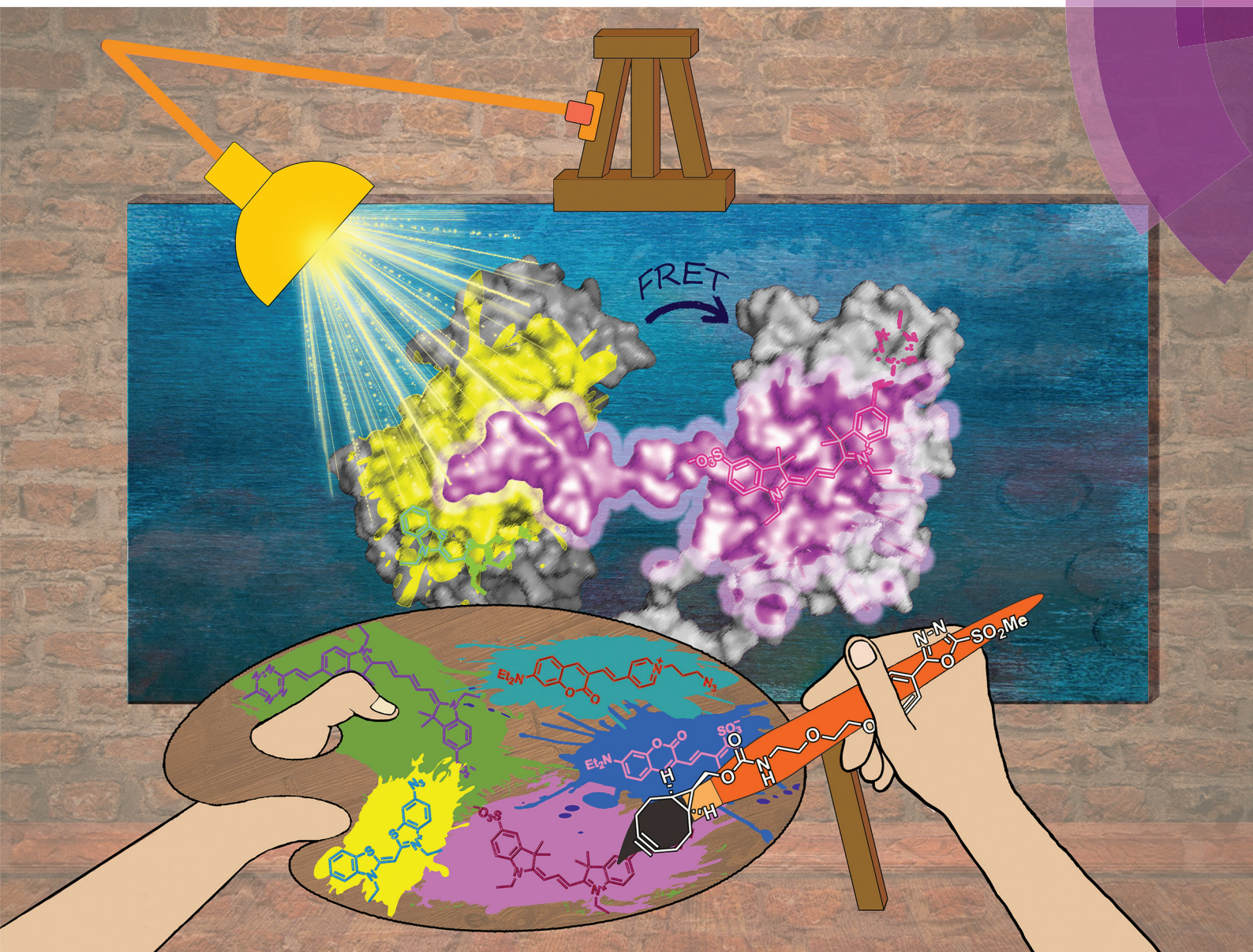


Organic & Biomolecular Chemistry

rsc.li/obc



ISSN 1477-0520



ROYAL SOCIETY
OF CHEMISTRY

PAPER

K. Németh *et al.*

Tracking down protein–protein interactions via a FRET-system using site-specific thiol-labeling



Cite this: *Org. Biomol. Chem.*, 2018, **16**, 5756

Tracking down protein–protein interactions *via* a FRET-system using site-specific thiol-labeling†

B. Sövegés,^a T. Imre,^b Á. L. Póti,^c P. Sok,^c Zs. Kele,^a A. Alexa,^c P. Kele ^a and K. Németh ^{*a}

Förster resonance energy transfer is among the most popular tools to follow protein–protein interactions. Although limited to certain cases, site-specific fluorescent labeling of proteins *via* natural functions by means of chemical manipulations can redeem laborious protein engineering techniques. Herein we report on the synthesis of a heterobifunctional tag and its use in site-specific protein labeling studies aiming at exploring protein–protein interactions. The oxadiazole-methylsulfonyl functionality serves as a thiol specific warhead that enables easy and selective installation of fluorescent labels through a bioorthogonal motif. Mitogen activated protein kinase (MAPK14) and its substrate mitogen activated protein kinase activated kinase (MAPKAP2) or its docking motif, a 22 amino acid-long peptide fragment, were labeled with a donor and an acceptor, respectively. Evolution of strong FRET signals upon protein–protein interactions supported the specific communication between the partners. Using an efficient FRET pair allowed the estimation of dissociation constants for protein–protein and peptide–protein interactions (145 nM and 240 nM, respectively).

Received 29th March 2018,
Accepted 19th June 2018

DOI: 10.1039/c8ob00742j

rsc.li/obc

Introduction

The human genome consists of nearly 30 000 genes, coding over half a million proteins. According to current estimations *ca.* 80% of proteins operate in complexes.¹ Understanding the interactions in such protein complexes is important in the exploration of biochemical processes *e.g.* antibody–antigen interactions, signal transduction and regulation or hormone-receptor binding.² Nowadays many robust methods are available for the detection of protein–protein interactions (PPI) (*e.g.*, affinity blotting, immunoprecipitation, quantitative proteomics, chemical crosslinking).^{3,4} To investigate protein communication in live cells, however, fluorescence methods *e.g.*

bimolecular fluorescence complementation (BiFC)^{5,6} or Förster resonance energy transfer (FRET) are the methods of choice.

Due to the time requirement for the reporter protein to mature BiFC cannot provide real-time information on PPIs, not to mention that the reconstituted fluorescent protein (FP) remains stable; thus the interaction is irreversible making BiFC less suitable to determine the dynamic features or spatio-temporal changes.⁷

The phenomenon of FRET is a highly distance-dependent process where an excited-state donor molecule transfers its energy to the acceptor molecule *via* non-radiative, coulombic interactions. Because the efficiency of FRET is inversely proportional to the sixth power of the distance between the donor and the acceptor, it proves to be a very sensitive and dynamic tool for the investigation and characterization of the dynamics of protein–protein interactions.^{8,9}

Selective fluorescence modulation of the proteins of interest can be considered one of the major challenges in the FRET technology. Fused FPs overcome this limitation in terms of selectivity; however, the comparable size of the fusion tags often hamper the dynamics of the interaction studied. Selective fluorescent tagging with small organic reporters can be achieved by the use of smaller fusion tags (SNAP, CyS₄ *etc.*) or by encoding fluorescent or bioorthogonalized non-canonical amino acids.¹⁰ While these techniques are powerful they are often laborious and require special skills and advanced infrastructure. In certain cases, purely chemical modification can be effected *e.g.* with reagents harboring a warhead that

^aResearch Centre for Natural Sciences of the Hungarian Academy of Sciences, Institute of Organic Chemistry, Chemical Biology Research Group, Magyar tudósok krt. 2, H-1117 Budapest, Hungary. E-mail: nemeth.krisztina@ttk.mta.hu; Tel: +36 1 382 6659

^bResearch Centre for Natural Sciences of Hungarian Academy of Sciences, Instrumentation Center, MS Metabolomics Research Group, Magyar tudósok krt. 2., H-1117 Budapest, Hungary

^cResearch Centre for Natural Sciences of the Hungarian Academy of Sciences, Institute of Enzymology, Protein Research Group, Magyar tudósok krt. 2, H-1117 Budapest, Hungary

† Electronic supplementary information (ESI) available: Accessible surface area calculations, *K_d* calculation, mass spectrometric analysis of labeled proteins, spectral overlap of the fluorescent proteins, NMR spectra of the synthetic products. See DOI: 10.1039/c8ob00742j



selectively targets rare functions.¹¹ Among the 20 protein-building amino acids, cysteine is one of the most suitable targets for such selective reactions because of the low abundance and good nucleophilicity of the free sulfhydryl group.¹² Hence, various methods were developed for cysteine bioconjugation,¹³ such as reactions with electrophiles (α -halo carbonyl derivatives),¹⁴ use of Michael acceptors (maleimide derivatives,¹⁵ vinyl sulfone¹⁶), thiol-yne or -ene reactions,¹⁷ disulfide exchange,¹⁸ nucleophilic aromatic substitution of perfluorobenzene derivatives,¹⁹ or use of allenamide derivatives.²⁰ The majority of these approaches suffer from some limitations, such as some of the reagents being able to also modify other nucleophilic amino acid side chains. In the case of Michael-acceptors the resulting products are often unstable, due to retro-Michael reactions or in the case of maleimides due to the fact that the maleimide linkage is prone to hydrolysis.¹³ Moreover, the thioether group suffers from reversible exchange reactions with reactive thiols. Disulfide conjugates also tend to participate in exchange reactions,²¹ while traditional thiol-ene reactions require nucleophilic or UV-light activation.²² The vinyl sulfone derivatives successfully addressed these problems; however, their reaction kinetics is still too slow for certain *in vivo* biological experiments.²³ Recently, Toda and co-workers investigated the Julia-Kocienski-like methylsulfonyl-functionalized heteroaromatic derivatives and presented a new thiol-selective reagent, which was stable in biological environments and offered superior reaction kinetics compared to other thiol-specific reactions.²⁴

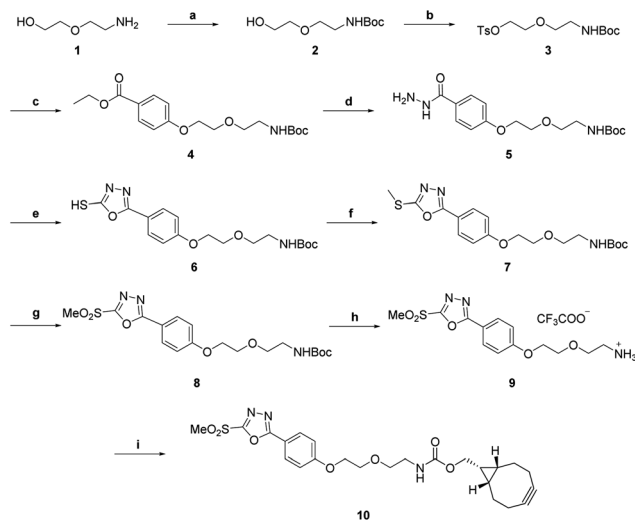
In this study, we aimed at investigating protein-protein interactions using FRET as an indicator of the communication of model protein p38 α (MAPK14) and its direct substrate MK2 (MAPKAP2). Both proteins are the key components of the mitogen-activated protein kinase signaling pathway.²⁵ p38 α is the main transponder of the inflammatory response, and MK2 plays an important role in the production of inflammatory cytokines.²

Based on our previous studies²⁶ with p38 and calculations of solvent accessible surface areas of the proteins, both of them contain accessible cysteines on their surface regions. Along the above considerations we designed a bifunctional chemical reporter tag carrying a thiol-reactive oxadiazole-methylsulfone and a bioorthogonally reactive cyclooctyne motif that creates a platform for fluorescent modification. The fluorescently labeled protein constructs were then used in the exploration of protein-protein interactions using FRET.

Results and discussion

Synthetic procedures

First, we wanted to screen for FRET pairs from our azide and tetrazine derivatized dye-pool.^{27–30} Since photophysical characteristics may substantially change upon conjugation to proteins, we needed a heterobifunctional tag that would enable Cys-specific targeting on the one hand and allow sequential one-pot high yielding modification both with azide- and tetra-



Scheme 1 Reaction conditions: (a) Boc₂O, DCM, 0–25 °C, 14 h, 96%; (b) TsCl, Et₃N, DCM, 25 °C, 14 h, quant.; (c) ethyl 4-hydroxybenzoate, K₂CO₃, DMF, 60 °C, 14 h, 99%; (d) N₂H₄ × H₂O, EtOH, Δ, 6 h, 99%; (e) CS₂, KOH, EtOH, 85 °C, 14 h, 87%; (f) CH₃I, Et₃N, THF, 25 °C, 2 h, quant.; (g) *m*CPBA, DCM, 0–25 °C, 14 h, 84%; (h) TFA, H₂O, DCM, 25 °C, 1 h, 99%; and (i) BCN-NHS, EDIPA, DCM, 0–25 °C, 90 min, 25%.

zine-modified fluorescent probes. To this end we designed cyclooctyne bearing methylsulfonyl-oxadiazole **10** (Scheme 1). The synthesis started with Boc-protection of aminoethoxyethanol, **1**, followed by the activation of the hydroxyl group with tosyl-chloride to provide **3**. The product was reacted with ethyl-hydroxybenzoate under basic conditions to obtain **4** in excellent yields. Hydrazide **5** was accessed upon treatment of **4** with hydrazine monohydrate.

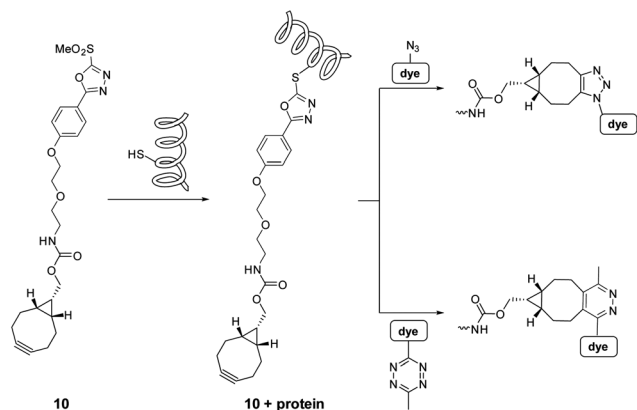
Oxadiazole **6** was then formed in good yields by a reaction of hydrazide **5** with carbon disulfide. Methylation of the sulfhydryl moiety was effected by treatment of **6** with methyl iodide to furnish **7**. Oxidation of **7** with *m*-chloroperoxybenzoic acid gave **8**. Acidic removal of the Boc-protecting group quantitatively afforded amine **9**. Compound **9** was functionalized with commercially available BCN-NHS to result in the Cys-specific heterobifunctional linker **10**.

Protein labeling and FRET pair screening

For protein-protein interactions we chose a mutant variant of p38 α where the cysteine at position 162 was replaced by serine (p38^{C162S}). This site should remain minimally perturbed, as it is located near the docking site of the protein. For an interacting partner we selected its downstream substrate, the wild type MAPKAP2 (MK2). Besides mutant p38^{C162S} and MK2 we extended our study to a 22 amino acid oligopeptide representing the docking motif of MK2 (CQIKIKKIEDASNPLLLKRRKK, pepMK2).²⁵

In order to screen for potential FRET pairs, we aimed at comparing the excitation and emission spectra of our dyes in their conjugate forms. To this end, we created a bioorthogonally targetable protein scaffold using heterobifunctional tag **10**, and p38^{C162S} (Scheme 2).





Scheme 2 Sequential chemical labeling strategy using the heterobifunctional linker and the bioorthogonalized fluorescent dyes.

Before labeling, we confirmed that **10** reacts solely with sulfhydryls. To do so we allowed **10** to react with glutathione (GSH). MS measurements (Fig. S1†) affirmed that only the SH-group participated in the reaction and no N-terminal modification was observed. These results are in agreement with the conclusions of Toda *et al.*²⁴

Intact whole protein MS measurements verified that complete conversion of p38^{C162S} could be achieved within 10 minutes by adding 2 equivalents of **10** to the protein, resulting in a mono-conjugated form of p38^{C162S} with a negligible amount of any multiply labeled species (Fig. S2 and 3†).

In order to identify the labeling site, tandem mass-spectrometry measurements were performed following trypsin digestion of p38^{C162S} treated with **9** (Fig. S11†). A comparison of untreated and derivatized p38^{C162S} samples revealed that the linker reacted mainly at Cys119, which is in accordance with our former results on calculated accessible surface area values (Table S1†).²⁶

Next, we wanted to screen for the most promising FRET pairs in our bioorthogonal dye-pool. For this, we applied the bifunctional, cyclooctyne bearing chemical reporter **10** on mutant p38 in sequential labeling experiments with a series of azide or tetrazine bearing fluorescent or fluorogenic dyes (**11–15**). The labeling reactions were conducted in one-pot with sequential administration of **10** and the respective dyes to the solution of p38^{C162S}, without any intermediate purification steps. Such bioorthogonal conjugation of the dyes was very efficient and in each case the conversion rates reached *ca.* 100% within 10 minutes, according to intact protein MS analyses (Fig. S2–8†). Due to the fluorogenic nature of the dyes, no non-specific signal was observed even if non-specific adhesion of the dyes onto the surface of the proteins occurred (Table S3†). The labeled proteins were separated using SDS-PAGE and imaged under different excitation sources. In each case the dyes labeled the protein successfully (Fig. 1).

Next, we analyzed the excitation and emission spectra of the dye–protein conjugates to identify donor–acceptor pairs with overlapping emission and excitation bands. After evaluat-

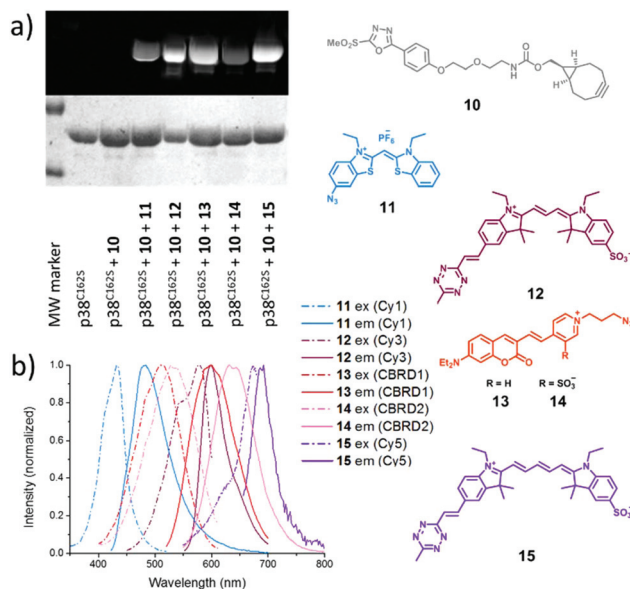


Fig. 1 (a) Fluorescent labeling of linker (**10**) tagged p38^{C162S} with bioorthogonalized dyes (**11–15**) monitored by SDS-PAGE. The upper gel refers to the fluorescence emission at different wavelengths (**11**: 488/520; **12**: 532/580; **13–14**: 488/610; and **15**: 633/670). The lower gel shows the result of the Coomassie staining. (b) Excitation and emission spectra of the listed dyes conjugated to p38^{C162S}.

ing the spectra, we identified a potential FRET pair of **11–12** (Fig. S13a†).

The efficiency and selectivity of the conjugation of **10** to MK2 were also assessed. In this case, addition of 2 equivalents of **10** to MK2 resulted in mono- and double-conjugated species as seen from intact whole protein MS measurements (Fig. S10†). Comparative MS-analysis of labeled and unlabeled, trypsin digested MK2 samples revealed that the two most accessible cysteines *i.e.*, Cys224 and Cys98 were involved (Table S2†).

FRET measurements

To explore the FRET efficiency between **11** (Cy1) and **12** (Cy3), the interacting partners were modified with the dyes applying the same sequential scheme using **10** as a heterobifunctional linker (Scheme 2). This way, mutant p38 was labeled with **11**, while MK2 and pepMK2 were tagged with **12** (Fig. S12†).

Following the purification of the fluorescently labeled proteins and peptide, we studied the interaction between Cy1-conjugated p38^{C162S} and Cy3-conjugated pepMK2 or MK2. The FRET interaction between labeled p38^{C162S} (0.5 μM) and increasing amounts of pepMK2 (0 to 8 μM) was monitored upon excitation of the donor fluorophore ($\lambda_{exc} = 420$ nm). The evolution of the FRET signal resulted in a gradual decrease of the donor fluorescence with a simultaneous increase of the acceptor's fluorescence (Fig. 2). FRET efficiency was calculated using the below equation:

$$E_{\text{FRET}} = 100(1 - D/D_0),$$



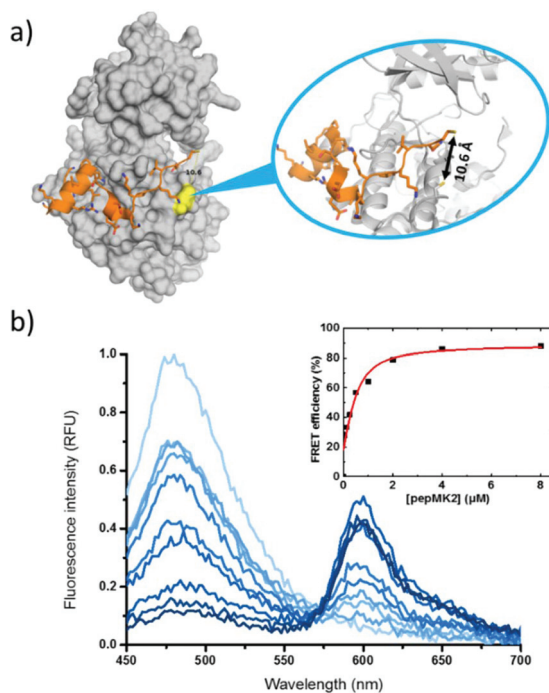


Fig. 2 (a) The structure of the complex of protein p38^{C162S} (based on PDB code 2OZA) and peptide MK2. The accessible cysteines are highlighted in yellow. (b) Changes in fluorescence upon interaction between the Cy1-labeled p38^{C162S} and Cy3-labeled peptide MK2 (inset shows the calculated FRET-efficiency).

where D is the fluorescence intensity of the donor in the presence of the acceptor at 482 nm at different concentrations and D_0 is the fluorescence intensity of the donor, in the absence of the acceptor. As seen in the inset of Fig. 2b the curve reached the saturation value at a remarkably high, 87% FRET-efficiency. This high FRET signal is in good accordance with the estimated short distance (10.6 Å) of the pepMK2 cysteine and the labeled Cys119 in p38 (according to the structure of the protein PDB code 2OZA).³¹ The dissociation constant ($K_d = 240$ nM; see the ESI†) for pepMK2 was calculated to be slightly higher than the literature data (*i.e.* 50 nM) obtained for wild type p38 α .²⁵ The difference can be attributed to the altered interactions caused by mutation at position 162 of p38 as well as the presence of the additional Cys residue at the N-terminal of the peptide. Differences in the measurement methods can also be the reason *e.g.*, fluorescence *vs.* polarization. Systematic comparative measurements supported this hypothesis (for more details *cf.* ESI part S7†).

In the case of the protein-protein interactions similar conditions were applied (Fig. 3). Signal changes were monitored at the same wavelengths upon interaction of fluorescently labeled Cy1-p38^{C162S} with increasing amounts of Cy3-labeled MK2 (0 to 4 μ M). For the calculation of the FRET efficiency the same equation was used; however, effects of protein interaction on donor fluorescence were taken into account as the presence of MK2 creates a less-polar environment for the donor resulting in an increase of the fluorescence intensity. Thus, the fluo-

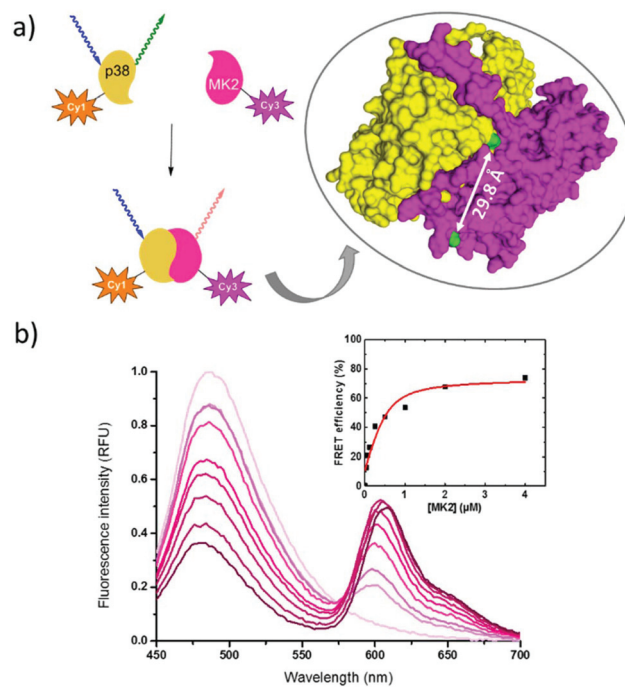


Fig. 3 (a) The structure of the complex of protein p38^{C162S} and protein MK2 (based on PDB code 2OZA). The accessible cysteines are highlighted in green. (b) The FRET signal between Cy1-labeled p38^{C162S} and Cy3-labeled protein MK2 (inset shows the calculated FRET-efficiency).

rescence intensity of the donor fluorophore in the presence of acceptor labeled MK2 was always normalized with the fluorescence intensity of the donor, in the presence of unlabeled MK2 at the respective concentrations (Fig. S15†). The FRET efficiency went to saturation at 74% (Fig. 3b). Both cysteines were located within the critical distance *i.e.*, 100 Å necessary for efficient FRET ($d_{\text{Cys224}} = 29.8$ Å and $d_{\text{Cys98}} = 23.7$ Å according to the structure of the protein complex PDB code 2OZA).³¹ The decreased FRET efficiency compared to the p38^{C162S}-pepMK2 interaction could be explained by the longer distance between the labeling sites. The binding affinity between p38 and MK2 protein was found to be $K_d = 145$ nM (see the ESI†). Estimated K_d values in the literature vary between 1 and 100 nM depending on the amino acid sequence, the size of the given fragment, the activity (phosphorylation) state of the interacting molecules and the ionic strength of the media.³²

The high salt concentration – applied in order to prevent the aggregation of MK2 – was concomitant of lower affinity in our setup.

Conclusions

In conclusion, we demonstrated the synthesis and use of a heterobifunctional linker that enables highly specific and efficient modification of proteins *via* free-sulfhydryl functionalities of cysteine residues through its methylsulfonyl-oxadiazole warhead. The cyclooctyne functionalized bifunctional methyl-



sulfonyl linker readily creates a bioorthogonal platform that offers easy and high-yielding modification with azide or tetrazine modified fluorescent probes. First, we used this heterobifunctional linker to screen for possible FRET pairs from our existing bioorthogonalized fluorescent pool. Following the identification of a promising FRET pair, we used this Cys-specific linker to modify p38^{C162S} and its interacting partner MK2 or its docking motif pepMK2 with a FRET donor and acceptor, respectively. Tandem-MS measurements verified the selective and specific labeling of both protein components. FRET studies involving donor and acceptor labeled p38^{C162S}-MK2 or p38^{C162S}-pepMK2 partners confirmed the specific interactions of the proteins. Such heterobifunctional linkers are suitable for the selective modification of proteins possessing accessible free sulfhydryl functionalities. On the other hand, the high FRET efficiency between the identified dye pairs (*ca.* 80%) is suitable for the detection of protein-protein interactions and estimation of the strength of affinity.

Experimental

Organic syntheses

General methods. Unless otherwise indicated, all starting materials were obtained from commercial suppliers (Sigma-Aldrich, Fluka, Merck, Alfa Aesar, Reanal, Molar Chemicals, Fluorochem) and used without further purification. The fluorogenic dyes (**11–15**) were prepared as described previously. Analytical thin-layer chromatography (TLC) was performed on silica gel 60 F254 precoated aluminium TLC plates from Merck. Visualization of TLC samples was performed using a 254/365 nm UV lamp and/or KMnO₄ stain. Column chromatography was carried out with silica gel (0.06–0.2 mm) purchased from Zeochem. Ratios of the solvents for the eluents are given in volumes (mL/mL). Flash column chromatography was performed on a CombiFlash Rf+System (Teledyne ISCO, Lincoln, NE, USA). NMR spectra were recorded on Varian Inova 500 MHz and Varian 600 MHz NMR spectrometers. Chemical shifts (δ) are given in parts per million (ppm) using solvent signals as the reference. Coupling constants (*J*) are reported in hertz (Hz). Splitting patterns are designated as s (singlet), d (doublet), t (triplet), qr (quadruplet), qv (quintuplet), m (multiplet), dd (doublet of a doublet), td (triplet doublet), dt (doublet triplet), and brs (broad singlet). The exact masses were determined using an Agilent 6230 time-of-flight mass spectrometer. All melting points were measured on an OptiMelt Automated Melting Point System and are uncorrected.

Synthesis of tert-butyl (2-(2-hydroxyethoxy)ethyl)carbamate (2). To a solution of 2-(2-aminoethoxy-ethan-1-ol) (1.04 mL; 10.37 mmol) in CH₂Cl₂ (60 mL) di-*tert*-butyl-dicarbonate (2.26 g; 10.37 mmol) was added, and the reaction mixture was stirred at room temperature for 18 h. After the evaporation of the solvent the crude product was purified by silica gel column chromatography (hexane/ethyl acetate = 1/3) to yield 2.05 g product as a colorless oil (96%). *R*_f = 0.29 (hexane/ethyl acetate

= 1/1). ¹H NMR (500 MHz, CDCl₃) δ 3.71–3.68 (m, 2H), 3.55–3.50 (m, 4H), 3.29 (t, *J* = 5.1 Hz, 2H), 1.41 (s, 9H). ¹³C NMR (126 MHz, CDCl₃) δ 156.3, 79.5, 72.4, 70.4, 61.8, 40.6, 28.5 (Fig. S16[†]). HRMS: [M + Na]⁺ calcd for [C₉H₁₉NO₄Na]⁺ *m/z* 228.1212, found *m/z* 228.1211.

2-(2-((tert-butoxycarbonyl)amino)ethoxy)ethyl 4-methylbenzenesulfonate (3). A solution of **2** (2.05 g; 10 mmol) and triethylamine (4.9 mL; 35 mmol) in CH₂Cl₂ (25 mL) was cooled to 0 °C. *p*-Toluenesulfonyl chloride (5.72 g; 30 mmol) dissolved in CH₂Cl₂ (10 mL) was added and the reaction mixture was allowed to warm to room temperature and stirred for 18 hours. Solids were filtered out and the filtrate was washed with 10% citric acid (3 × 100 mL) and brine (1 × 100 mL) and dried over MgSO₄. After filtration the solvent was removed *in vacuo* and the crude product was purified by silica gel column chromatography (hexane/ethyl acetate = 3/1) to yield 6.13 g (68%) of a colorless oil. *R*_f = 0.54 (hexane/ethyl acetate = 1/1). ¹H NMR (500 MHz, CDCl₃) δ 7.79 (d, *J* = 8.2 Hz, 2H), 7.34 (d, *J* = 8.0 Hz, 2H), 4.78 (s, 1H), 4.16–4.13 (m, 2H), 3.63–3.60 (m, 2H), 3.43 (t, *J* = 5.1 Hz, 2H), 3.22 (t, *J* = 4.8 Hz, 2H), 2.43 (s, 3H), 1.43 (s, 9H). ¹³C NMR (126 MHz, CDCl₃) δ 156.0, 145.0, 133.2, 129.9, 128.1, 79.5, 70.5, 69.2, 68.5, 40.4, 28.5, 21.7 (Fig. S17[†]). HRMS: [M + Na]⁺ calcd for [C₁₆H₂₅NO₆SNa]⁺ *m/z* 382.1300, found *m/z* 382.1296.

Synthesis of ethyl 4-(2-(2-((tert-butoxycarbonyl)amino)ethoxy)ethoxy)benzoate (4). Ethyl 4-hydroxybenzoate (0.92 g, 5.54 mmol), compound **3** (2.00 g, 5.54 mmol) and dry K₂CO₃ (2.30 g, 16.62 mmol) were dissolved in anhydrous DMF (20 mL) under a N₂ atmosphere and stirred overnight at 60 °C. After cooling down the reaction mixture was diluted with 80 mL CH₂Cl₂ and washed with 3 × 80 mL water, 80 mL brine and dried over MgSO₄. After evaporation of the solvent the crude product was purified by silica gel column chromatography with hexane/ethyl acetate = 10/1–1/1 to yield 1.94 g (99%) product as white crystals. *R*_f = 0.67 (hexane/ethyl acetate = 1/1). Mp = 48–52 °C. ¹H NMR (500 MHz, CD₃OD): δ 8.03 (d, *J* = 8.9 Hz, 2H), 7.09 (d, *J* = 8.9 Hz, 2H), 4.40 (q, *J* = 7.1 Hz, 2H), 4.29–4.26 (m, 2H), 3.92–3.89 (m, 2H), 3.65 (t, *J* = 5.7 Hz, 2H), 3.32 (t, *J* = 5.6 Hz, 2H), 1.50 (s, 9H), 1.44 (t, *J* = 7.1 Hz, 3H). ¹³C NMR (126 MHz, CDCl₃) δ 166.5, 162.5, 133.0, 131.7, 123.4, 114.3, 110.2, 70.7, 69.4, 67.6, 60.8, 57.8, 28.6, 14.5 (Fig. S18[†]). HRMS: [M + Na]⁺ calcd for [C₁₈H₂₇NO₆Na]⁺ *m/z* 376.1736, found *m/z* 376.1735.

Synthesis of tert-butyl (2-(2-(4-(hydrazinecarbonyl)phenoxy)ethoxy)ethyl)carbamate (5). In a round-bottomed flask **4** (1.92 g; 5.44 mmol) and hydrazine monohydrate (792 μ L; 16.32 mmol) were heated under reflux for 30 min. Then ethanol was added (1.3 mL) and the mixture was stirred at the reflux temperature for 6 hours. After evaporation of the solvent the residue was purified by silica gel column chromatography (ethyl acetate/MeOH = 20/1) to give **5** as a colorless oil (1.83 g, 99%). *R*_f = 0.31 (ethyl acetate/MeOH = 20/1). ¹H NMR (500 MHz, DMSO-*d*₆): δ 7.82 (d, *J* = 8.6 Hz, 2H), 7.14 (d, *J* = 8.8 Hz, 2H), 6.75 (t, *J* = 5.3 Hz, 1H), 4.21–4.17 (m, 2H), 3.77–3.73 (m, 2H), 3.46 (t, *J* = 6.0 Hz, 2H), 3.09 (q, *J* = 6.0 Hz, 2H), 1.37 (s, 9H). ¹³C NMR (126 MHz, CDCl₃) δ 168.2, 161.7, 156.1, 128.9,



125.2, 114.6, 70.6, 69.3, 67.6, 50.7, 40.4, 28.5 (Fig. S19[†]). HRMS: $[M + H]^+$ calcd for $[C_{16}H_{26}N_3O_5]^+$ m/z 340.1872, found m/z 340.1863.

Synthesis of tert-butyl (2-(2-(4-(5-mercapto-1,3,4-oxadiazol-2-yl)phenoxy)ethoxy)ethyl)carbamate (6). To a solution of **5** (2.00 g, 5.88 mmol) in ethanol (14 mL) carbon disulfide (2.34 mL, 38.81 mmol) and KOH (330 mg, 5.88 mmol) were added and the solution was stirred at 85 °C overnight. After cooling to room temperature, the mixture was diluted with ethyl acetate (100 mL) and washed with 1 M HCl (2 × 80 mL) and brine (100 mL) and dried over MgSO₄. The crude product was purified by silica gel column chromatography (hexane/ethyl acetate = 2/1–1/9) to yield 1.95 g (87%) of a white solid. R_f = 0.57 (hexane/ethyl acetate = 1/9). Mp = 76–82 °C. ¹H NMR (500 MHz, CDCl₃): δ 12.51 (s, 1H), 7.75 (d, J = 8.1 Hz, 2H), 6.95 (d, J = 8.6 Hz, 2H), 5.21 (s, 1H), 4.23–4.14 (m, 2H), 3.87 (d, J = 4.0 Hz, 2H), 3.66 (t, J = 5.0 Hz, 2H), 3.39 (s, 2H), 1.45 (s, 9H). ¹³C NMR (126 MHz, CDCl₃) δ 177.8, 161.8, 156.5, 128.9, 128.2, 116.3, 115.1, 70.4, 69.2, 67.5, 40.3, 28.4, 11.4 (Fig. S20[†]). HRMS: $[M + Na]^+$ calcd for $[C_{17}H_{23}N_3O_5SNa]^+$ m/z 404.1256, found m/z 404.1263.

Synthesis of tert-butyl (2-(2-(4-(5-(methylthio)-1,3,4-oxadiazol-2-yl)phenoxy)ethoxy)ethyl)carbamate (7). Compound **6** (3.03 g, 7.93 mmol) was dissolved in THF (50 mL) and cooled to 0 °C. Then CH₃I (592 μL, 9.52 mmol) and Et₃N (1.33 mL, 9.52 mmol) were added and the mixture was stirred for 2 h at room temperature. After evaporation of the solvent ethyl acetate was added (200 mL) and the mixture was extracted with water (3 × 100 mL). The water phase was washed with ethyl acetate (2 × 100 mL). The combined organic phase was washed with brine (200 mL) and dried over MgSO₄. The crude product was dissolved in Et₂O (10 mL), and hexane was added dropwise. The solvents were removed using a pipette from the pale yellow oil formed and it was washed again. After evaporation to dryness the product appeared as a white solid (3.14 g; 90%). R_f = 0.76 (ethyl acetate/methanol = 9/1); 0.25 (hexane/ethyl acetate = 1/1). Mp = 42–44 °C. ¹H NMR (500 MHz, CDCl₃): δ 7.91 (d, J = 8.9 Hz, 2H), 7.00 (d, J = 8.9 Hz, 2H), 4.96 (s, 1H), 4.18–4.14 (m, 2H), 3.85–3.81 (m, 2H), 3.60 (t, J = 5.1 Hz, 2H), 3.33 (d, J = 4.8 Hz, 2H), 2.74 (s, 3H), 1.42 (s, 9H). ¹³C NMR (126 MHz, CDCl₃): δ 165.8, 164.4, 161.5, 156.1, 128.5, 116.6, 115.2, 79.4, 70.6, 69.4, 67.7, 40.4, 28.5, 14.8 (Fig. S21[†]). HRMS: $[M + H]^+$ calcd for $[C_{18}H_{26}N_3O_5S]^+$ m/z 396.1583, found m/z 396.1593.

Synthesis of tert-butyl (2-(2-(4-(5-(methylsulfonyl)-1,3,4-oxadiazol-2-yl)phenoxy)ethoxy)ethyl)carbamate (8). Compound **7** (1.98 mg, 5.0 mmol) was dissolved in CH₂Cl₂ (40 mL), and cooled to 0 °C. *m*CPBA (70 wt%; 3.19 g; 18.5 mmol) was added and the mixture was stirred at room temperature overnight. After filtration of the insoluble material the solvent was evaporated, and the residue was purified by silica gel column chromatography (hexane/ethyl acetate = 2/1–ethyl acetate/MeOH = 9/1) which gave the title compound **8** (1.77 g, 84%) as a white solid. R_f = 0.25 (hexane/ethyl acetate = 1/1). Mp = 118–120 °C. ¹H NMR (500 MHz, DMSO-*d*₆): δ 8.03 (d, J = 8.8 Hz, 2H), 7.21 (d, J = 8.8 Hz, 2H), 6.76 (s, 1H), 4.26–4.19 (m,

2H), 3.79–3.74 (m, 2H), 3.69 (s, 3H), 3.47 (t, J = 6.0 Hz, 2H), 3.10 (q, J = 5.8 Hz, 2H), 1.37 (s, 9H). ¹³C NMR (126 MHz, DMSO-*d*₆): δ 165.7, 162.2, 161.6, 155.6, 142.0, 129.4, 115.5, 114.2, 77.5, 69.3, 68.4, 67.6, 42.9, 28.2 (Fig. S22[†]). HRMS: $[M + Na]^+$ calcd for $[C_{18}H_{25}N_3O_7SNa]^+$ m/z 450.1311, found m/z 450.1315.

Synthesis of 2-(2-(4-(5-(methylsulfonyl)-1,3,4-oxadiazol-2-yl)phenoxy)ethoxy)ethan-1-aminium 2,2,2-trifluoroacetate (9). To a solution of compound **8** (269 mg, 0.63 mmol) in CH₂Cl₂ (5 mL), H₂O (20 μL) and TFA (1 mL) were added and the mixture was stirred for 1 h at room temperature. After completion of the reaction (checked by TLC) the solvents were evaporated using N₂ and the crude product was washed with Et₂O (3 × 3 mL). The product precipitates as off-white crystals (240 mg, 80%). Mp = 146–148 °C. ¹H NMR (500 MHz, CD₃OD): δ 8.09 (d, J = 8.8 Hz, 2H), 7.19 (d, J = 8.8 Hz, 2H), 4.35–4.29 (m, 2H), 3.99–3.96 (m, 2H), 3.86–3.83 (m, 2H), 3.59 (s, 3H), 3.35 (s, 1H), 3.21 (t, J = 4.8 Hz, 2H). ¹³C NMR (126 MHz, CD₃OD) δ 168.0, 164.2, 163.5, 130.7, 116.5, 116.0, 70.6, 69.0, 68.1, 43.3, 40.7 (Fig. S23[†]). HRMS: $[M]^+$ calcd for $[C_{13}H_{18}N_3O_5S]^+$ m/z 328.0967, found m/z 328.0962.

Synthesis of bicyclo[6.1.0]non-4-yn-9-ylmethyl (2-(2-(4-(5-(methylsulfonyl)-1,3,4-oxadiazol-2-yl)phenoxy)ethoxy)ethyl)carbamate (10). Compound **9** (30 mg; 0.07 mmol) and EDIPA (35 μL; 0.20 mmol) were dissolved in CH₂Cl₂ (4 mL) and cooled to 0 °C. BCN-succinimidyl carbonate (24 mg; 0.08 mmol) was added and stirred for 3 h at room temperature. After evaporation of the solvent the residue was purified by flash chromatography using CH₂Cl₂/MeOH = 100/1–30/1 to yield the product (13 mg; 37%) as a colorless oil. R_f = 0.35 (CH₂Cl₂/MeOH = 30/1). ¹H NMR (500 MHz, CDCl₃) δ 8.06 (d, J = 8.9 Hz, 2H), 7.06 (d, J = 8.9 Hz, 2H), 5.06 (s, 1H), 4.22–4.19 (m, 2H), 4.14 (d, J = 8.0 Hz, 2H), 3.87–3.83 (m, 2H), 3.64 (t, J = 5.1 Hz, 2H), 3.50 (s, 3H), 3.40 (dd, J = 10.5, 5.2 Hz, 2H), 2.34–2.12 (m, 6H), 1.59–1.51 (m, 2H), 1.40–1.30 (m, 1H), 0.93 (t, J = 9.7 Hz, 2H). ¹³C NMR (126 MHz, CDCl₃) δ 162.9, 161.8, 156.9, 129.8, 128.9, 115.6, 114.8, 98.9, 70.6, 69.4, 67.9, 63.0, 53.9, 43.1, 29.2, 21.6, 20.3, 17.9 (Fig. S24[†]). HRMS: $[M + H]^+$ calcd for $[C_{24}H_{30}N_3O_7S]^+$ m/z 504.1804, found m/z 504.1797.

Peptide synthesis and protein expression and purification

Peptide MK2. The peptide was synthesized using a standard Fmoc-SPPS protocol. It was synthesized on Rink Amid MBHA resin (Protein Technologies, Inc.) using a peptide synthesizer (PS3, Protein Technologies, Inc.). Coupling reactions used Fmoc-L-amino acid/HBTU/NMM (5/4/10 eq.) in DMF (peptide synthesis grade). A cleaving solution of 5 mL of TFA/H₂O/TIS (95/2.5/2.5% v/v) was added to the resin, and mixed for 2 h. The crude peptide was purified using semi-preparative HPLC (Jupiter 10 μm C18300 Å, LC Column 250 × 10 mm; Phenomenex, Torrance, CA, USA).

MK2 protein. The cDNA of the MK2 human protein DNA construct containing residues between 41 and 400 was cloned into a modified pET expression vector. cDNA encoding the MK2 construct was produced from HEK293 derived mRNA. The MK2 construct was expressed in *Escherichia coli* Rosetta



(DE3) pLysS (Novagen) cells. The expressed MK2 construct contained an N-terminal cleavable GST-tag and a C-terminal uncleavable hexahistidine-tag. Protein purification involved two steps: Ni- and then GST-affinity chromatography. The GST tag was removed by tobacco etch virus protease. Finally, the MK2 protein was purified again by Ni-affinity chromatography to remove the cleaved GST.

p38^{C162S} protein. The protein expression was carried out according to our previously reported procedure.²³

Conjugation processes

Conjugation of model proteins and fluorescent linkers. In the case of p38^{C162S}, 60 μ M protein and 120 μ M linker **10** were mixed and incubated for 10 minutes at room temperature in the dark in PBS buffer (pH 7.4). In the second step, an appropriate dye (**11–15**) was added in 240 μ M concentration for 10 min, too. The excess reagents were removed by using a SpinPrep column (Sigma, St Louis, MO, USA) filled with Sephadex G-25 “Fine” desalting gel (Pharmacia Fine Chemicals, Sweden). In the case of MK2, 60 μ M protein and 120 μ M linker **10** were mixed and incubated for 10 minutes at room temperature in the dark in PBS buffer (pH 7.4) completed with additional 160 mM NaCl, 0.1% IGEPAL and 400 μ M TCEP. In the second step dye **12** was added. The excess reagents were removed by using a SpinPrep column filled with Sephadex G-25 “Fine” desalting gel.

Fluorescent conjugation of pepMK2. 500 μ M peptide, 1 mM TCEP and 3 mM of compound [**10 + 12**] were mixed and incubated for 1 hour at room temperature in the dark in 50 mM HEPES buffer (pH 8.0). It was purified by HPLC (Phenomenex Jupiter 10 μ m Proteo C18 90 Å, LC Column 250 \times 10 mm) using H₂O + 0.1% TFA as eluent A and CH₃CN + 0.1% TFA as eluent B and the product was lyophilized.

SDS polyacrylamide gel electrophoresis. The samples were diluted with a sample buffer (250 mM Tris-HCl (pH 6.8) + 10% SDS + 40% glycerol + 0.02% bromophenol blue + 400 mM DTT) in a 3 : 1 ratio. The size of the polyacrylamide gels was 8.5 cm \times 7.5 cm \times 0.1 cm. They were the combination of 4% concentration and 10% separation PAGE gels (acrylamide/bisacrylamide ratio was 29/1; and concentration gel buffer was 125 mM Tris-HCl + 0.1% SDS (pH 6.8) and the separation gel buffer was 375 mM Tris-HCl + 0.1% SDS (pH 8.8)). 7.5 μ g of protein was loaded per lane. A Prestained PAGERuler Plus (Thermo Fisher Scientific) was applied as the molecular weight standard. Separations were carried out in a Mini-Protean Tetra Cell (Bio-Rad, Hercules, CA, USA) using 25 mM Tris/192 mM glycine + 0.1% SDS (pH 8.3) as the running buffer and 180 V voltage for 40 min at 25 °C. The gels were documented by using a Typhoon Trio Imaging System (GE Healthcare, Uppsala, Sweden). Furthermore, the gels were stained for proteins with Coomassie Brilliant-Blue.

FRET measurements

The labeled p38^{C162S} samples were prepared in 1.0 μ M concentration in PBS (pH 7.4) buffer. The labeled MK2 peptide and protein samples were prepared in 16, 8, 4, 2, 1, 0.5, 0.25, 0.125,

0.0625, and 0.03125 μ M concentrations for the titration. From the appropriate solutions 10 + 10 μ L were transferred into the wells. The FRET interactions between the two labeled partners were monitored based on the generation of the fluorescence signal (λ_{ex} : 420 nm; λ_{em} : 450–700 nm) by using a PerkinElmer Enspire Multimode Reader (PerkinElmer Inc.; Waltham, MA, USA) in a 384-well round bottom black plate (Corning, Corning, NY, USA) at room temperature with 100 flashes per point. Data were acquired and handled by Corning Enspire Manager 4.10 software.

Conflicts of interest

There are no conflicts to declare.

Acknowledgements

The help of Gábor Glatz with SDS-PAGE gel imaging is greatly acknowledged. The present work was supported by the Hungarian Scientific Research Fund (OTKA-NN-116265), the “Lendület” Programme of the Hungarian Academy of Sciences (LP2013-55/2013) and the National Research, Development and Innovation Office, Hungary (VEKOP-2.3.3.-15-20016-00011).

References

- 1 T. Berggård, S. Linse and P. James, *Proteomics*, 2007, **7**, 2833–2842.
- 2 Y. Yang, H. Liu and X. Yao, *Mol. BioSyst.*, 2012, **8**, 2106–2118.
- 3 Y. Song, V. G. J. Rodgers, J. S. Schultz and J. Liao, *Biotechnol. Bioeng.*, 2012, **109**, 2875–2883.
- 4 E. M. Phizicky and S. Fields, *Microbiol. Rev.*, 1995, **59**, 94–123.
- 5 T. K. Kerppola, *Annu. Rev. Biophys.*, 2008, **37**, 465–487.
- 6 K. E. Miller, Y. Kim, W. Huh and H. Park, *J. Mol. Biol.*, 2015, **427**, 2039–2055.
- 7 S. Xing, N. Wallmeroth, K. W. Berendzen and C. Grefen, *Plant Physiol.*, 2016, **171**, 727–758.
- 8 D. W. Piston and G. J. Kremers, *Trends Biochem. Sci.*, 2007, **32**, 407–414.
- 9 H. Sahoo, *J. Photochem. Photobiol., C*, 2011, **12**, 20–30.
- 10 G. Zhang, S. Zheng, H. Liuc and P. R. Chen, *Chem. Soc. Rev.*, 2015, **44**, 3405–3417.
- 11 N. Krall, F. P. da Cruz, O. Boutureira and G. J. Bernardes, *Nat. Chem.*, 2016, **8**, 103–113.
- 12 X. Chen and Y.-W. Wu, *Org. Biomol. Chem.*, 2016, **14**, 5417–5439.
- 13 S. B. Gunnoo and A. Madder, *ChemBioChem*, 2016, **17**, 529–553.
- 14 J. M. Chalker, G. J. L. Bernardes, Y. A. Lin and B. G. Davis, *Chem. – Asian J.*, 2009, **4**, 630–640.



- 15 A. D. Baldwin and K. L. Kiick, *Bioconjugate Chem.*, 2011, **22**, 1946–1953.
- 16 G. B. Cserép, Zs. Baranyai, D. Komáromy, K. Horváti, Sz. Bősze and P. Kele, *Tetrahedron*, 2014, **70**, 5961–5965.
- 17 C. E. Hoyle and C. N. Bowman, *Angew. Chem., Int. Ed.*, 2010, **49**, 1540–1573.
- 18 S. van Kasteren, *Biochem. Soc. Trans.*, 2012, **40**, 929–944.
- 19 A. M. Spokoiny, Y. Zou, J. J. Ling, H. Yu, Y.-S. Lin and B. L. Pentelute, *J. Am. Chem. Soc.*, 2013, **135**, 5946–5949.
- 20 A. Abbas, B. Xing and T. P. Loh, *Angew. Chem., Int. Ed.*, 2014, **53**, 74914–77494.
- 21 J. M. Chalker, G. J. L. Bernardes and B. G. Davis, *Acc. Chem. Res.*, 2011, **44**, 730–741.
- 22 S. P. S. Koo, M. M. Stamenovic, R. A. Prasath, A. J. Inglis, F. E. Du Prez, C. Barner-Kowollik, W. van Camp and T. Junkers, *J. Polym. Sci., Part A: Polym. Chem.*, 2010, **48**, 1699–1713.
- 23 J. Morales-Sanfrutos, J. Lopez-Jaramillo, M. Ortega-Muñoz, A. Megia-Fernandez, F. Perez-Balderas, F. Hernandez-Mateo and F. Santoyo-Gonzalez, *Org. Biomol. Chem.*, 2010, **8**, 667–675.
- 24 N. Toda, S. Asano and C. F. Barbas III, *Angew. Chem., Int. Ed.*, 2013, **52**, 12592–12596.
- 25 Á. Garai, A. Zeke, G. Gógl, I. Törő, F. Fördős, H. Blankenburg, T. Bárkai, J. Varga, A. Alexa, D. Emig, M. Albrecht and A. Reményi, *Sci. Signaling*, 2012, **5**, ra74.
- 26 B. Söveges, T. Imre, T. Szende, Á. L. Póti, G. B. Cserép, T. Hegedús, P. Kele and K. Németh, *Org. Biomol. Chem.*, 2016, **14**, 6071–6078.
- 27 R. Petrovics, B. Söveges, A. Egyed, G. Knorr, A. Kormos, T. Imre, Gy. Török, A. Zeke, É. Kocsmár, G. Lotz, P. Kele and K. Németh, *Org. Biomol. Chem.*, 2018, **16**, 2997–3005.
- 28 G. Knorr, E. Kozma, J. M. Schaart, K. Németh, G. Török and P. Kele, *Bioconjugate Chem.*, 2018, **29**, 1312–1318.
- 29 P. Kele, X. Li, M. Link, K. Nagy, A. Herner, K. Lőrincz, Sz. Béni and O. S. Wolfbeis, *Org. Biomol. Chem.*, 2009, **7**, 3486–3490.
- 30 K. Nagy, E. Orbán, Sz. Bősze and P. Kele, *Chem. – Asian J.*, 2010, **5**, 773–777.
- 31 A. White, C. A. Pargellis, J. M. Studts, B. G. Werneburg and B. T. Farmer II, *Proc. Natl. Acad. Sci. U. S. A.*, 2007, **104**, 6353–6358.
- 32 S. M. Lukas, R. R. Kroe, J. Wildeson, G. W. Peet, L. Frego, W. Davidson, R. H. Ingraham, C. A. Pargellis, M. E. Labadia and B. G. Werneburg, *Biochemistry*, 2004, **43**, 9950–9960.

